Supporting Information

Si Containing Block Copolymers Quickly Assembly into Sub-6 nm Domains

Jianuo Zhou, Xuemiao Li, Zhenyu Yang and Hai Deng*

School of Microelectronics and State Key Laboratory of Molecular Engineering of Polymers, Fudan University, Shanghai 200433, China

1. Synthetic route and characterization of TMSS and StNPOSS monomer.

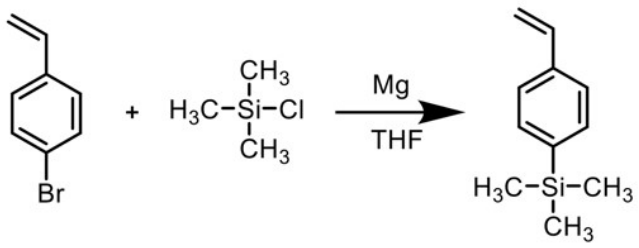

Scheme S1. Synthetic route of TMSS monomer.

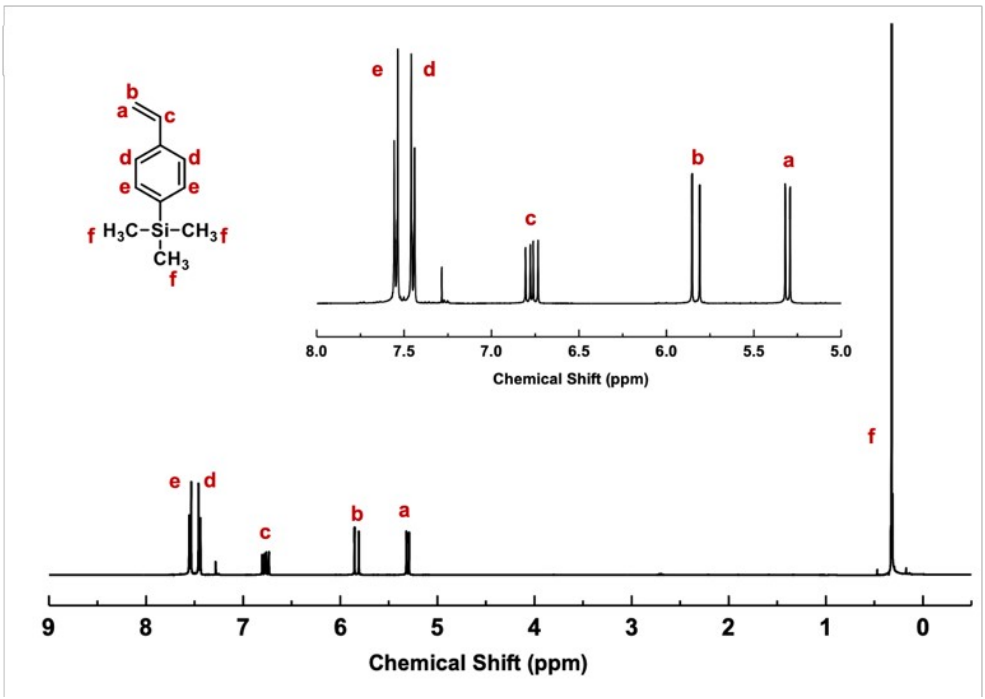

Figure S1. ^{1}H NMR spectrum of TMSS monomer. (400 MHz, $CDCl_3$)

^{1}H NMR (400 MHz, $CDCl_3$) δ 7.55 (d, *J* = 6.4 Hz, Ar-*H*, 2H), 7.45 (d, *J* = 6.4 Hz, Ar-*H*, 2H), 6.76 (dd, *J* = 14.4, 9.2 Hz, -*CH*=CH_2, 1H), 5.85 (d, *J* = 14.4 Hz, -CH=*CH_2*, 1H), 5.30 (d, *J* = 9.2 Hz, -CH=*CH_2*, 1H), 0.33 (s, -Si*$(CH_3)_3$*, 9H).

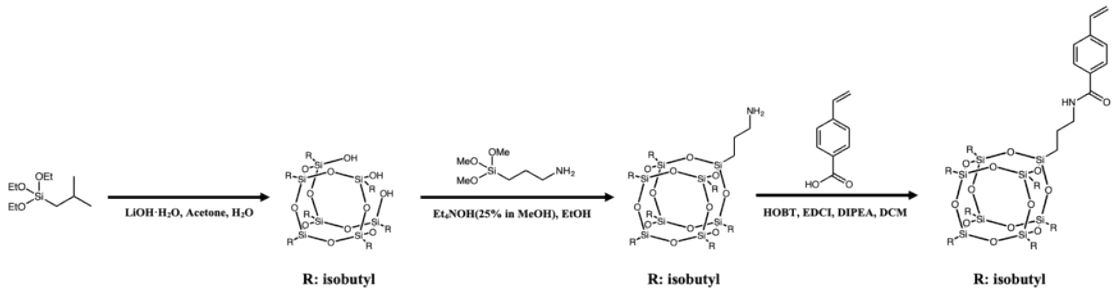

Scheme S2. Synthetic route of StNPOSS monomer.

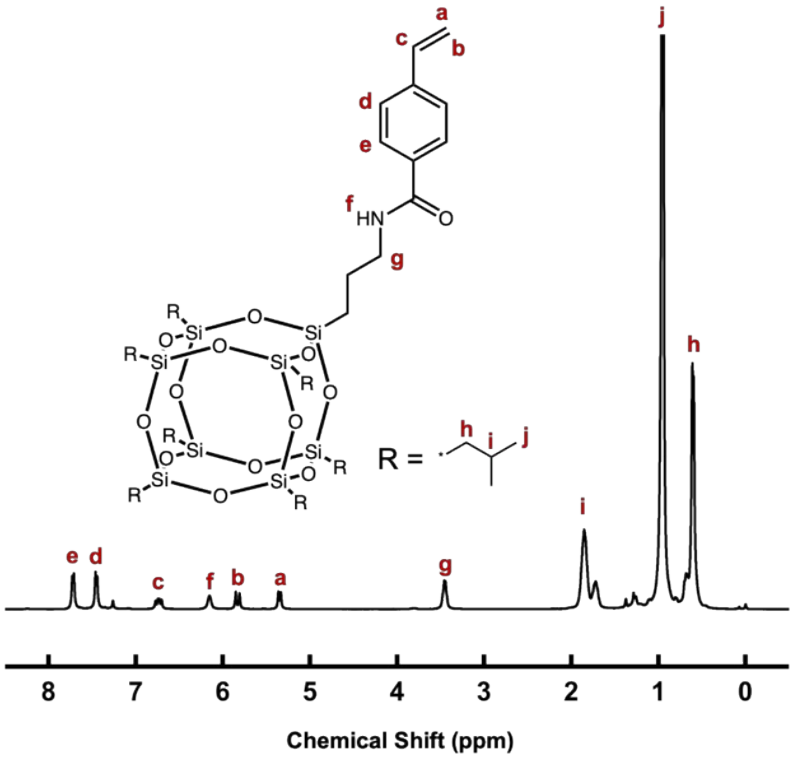

Figure S2. ^{1}H NMR spectrum of StNPOSS monomer. (400 MHz, $CDCl_3$)

^{1}H NMR (400 MHz, $CDCl_3$) δ 7.72 (d, *J* = 7.9 Hz, Ar-*H*, 2H), 7.45 (d, *J* = 7.9 Hz, Ar-*H*, 2H), 6.74 (dd, *J* = 17.6, 10.8 Hz, -*CH*=CH_2, 1H), 6.15 (s, -*NH*-, 1H), 5.83 (d, *J* = 17.6 Hz, -CH=*CH_2*, 1H), 5.35 (d, *J* = 10.8 Hz, -CH=*CH_2*, 1H), 3.45 (q, *J* = 6.7 Hz, -*CH2*-NH-, 2H), 1.86 (dq, *J* = 13.8, 6.7 Hz, -CH_2*CH*-, 7H), 1.72 (p, *J* = 7.2 Hz, -*CH_2*-CH_2-NH-, 2H), 0.95 (d, *J* = 6.6 Hz, -CH*$(CH_3)_2$*, 42H), 0.75 – 0.37 (m, Si-*CH_2*-, 16H).

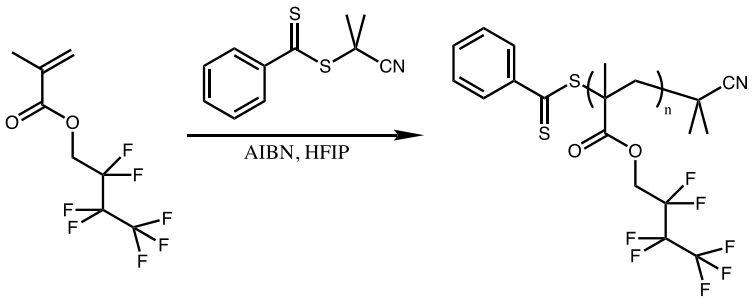

2. Synthesis and Characterization of Si- and F-containing BCPs.

Scheme S3. Synthetic route of PHFBMA homopolymer (macro-CTA).

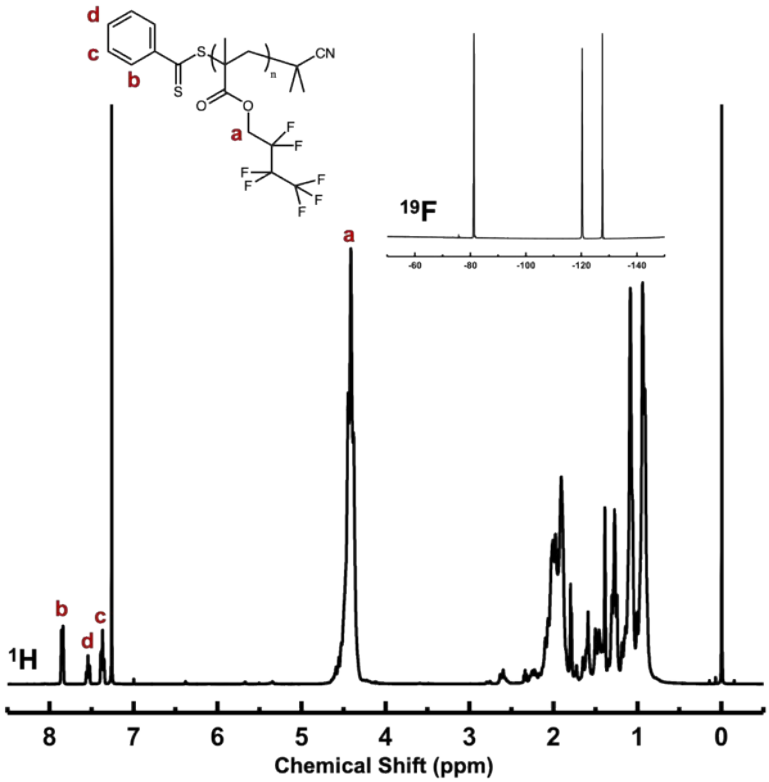

Figure S3. ^{1}H, ^{19}F NMR spectrums of PHFBMA homopolymer (macro RAFT CTA). (400 MHz, $CDCl_3$)

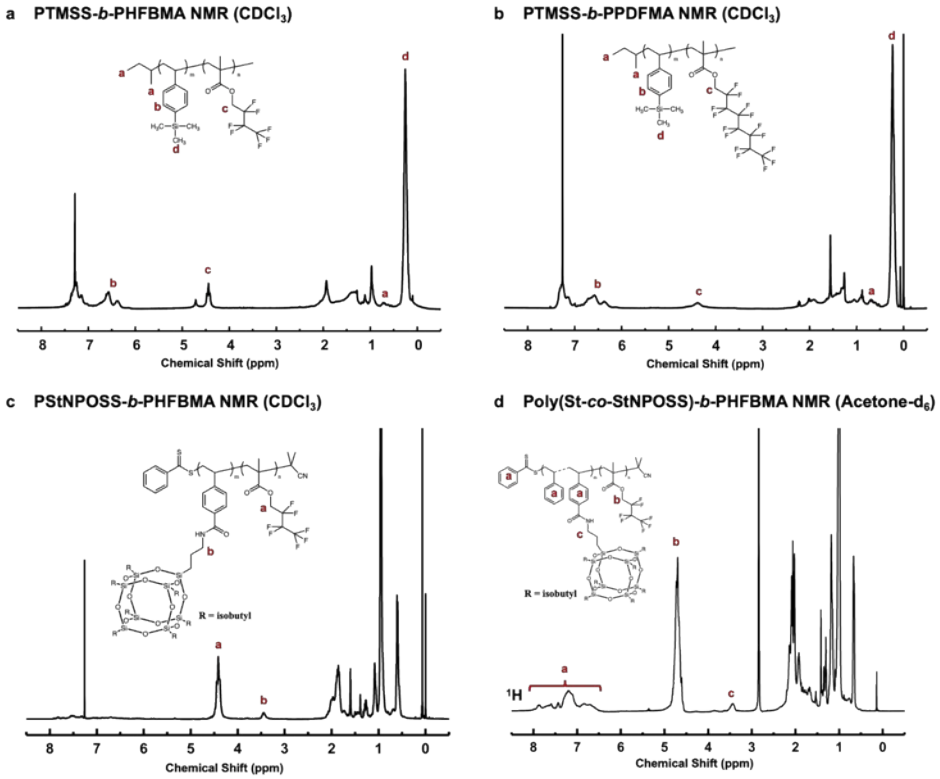

Figure S4. Full ^{1}H NMR spectrum of a) PTMSS-*b*-PHFBMA (400 MHz, $CDCl_3$), b) PTMSS-*b*-PPDFMA (400 MHz, $CDCl_3$), c) PStNPOSS-*b*-PHFBMA (400 MHz, $CDCl_3$) and d) Poly(St-*co*-StNPOSS)-*b*-PHFBMA (400 MHz, Acetone-d_6) block copolymer.

Table S1. Characterization of PStNPOSS-*b*-PHFBMA with shorter chain length.

Sample	Mn[a] ($kg \cdot mol^{-1}$)	PDI[a]	$DP_{StNPOSS}$[b]	DP_{HFBMA}[b]	*N*	Morphology[d]
$PStNPOSS_{1.5}$-*b*-$PHBMFA_{30}$	8.4	1.07	1.5	30	88	DIS
$PStNPOSS_{3.2}$-*b*-$PHBMFA_{30}$	8.7	1.09	3.2	30	104	DIS
$PStNPOSS_{6.3}$-*b*-$PHBMFA_{30}$	10.0	1.07	6.3	30	135	DIS
$PStNPOSS_{4.5}$-*b*-$PHBMFA_{25}$	8.8	1.08	4.5	25	105	DIS

a) The number-average molecular weights (M_n) and polydispersity indexes (PDI) were obtained by GPC in THF against PS standards. b) The degrees of polymerization of PStNPOSS-*b*-PHFBMA were calculated by ^{1}H-NMR. c) Calculation of the total degree of polymerization (N) was performed based on a 118 $Å^3$ reference volume (v_0) using the densities of PHFBMA (1.55 $g \cdot cm^{-3}$) and PStNPOSS (1.44 $g \cdot cm^{-3}$). d) Morphology was characterized by SAXS.

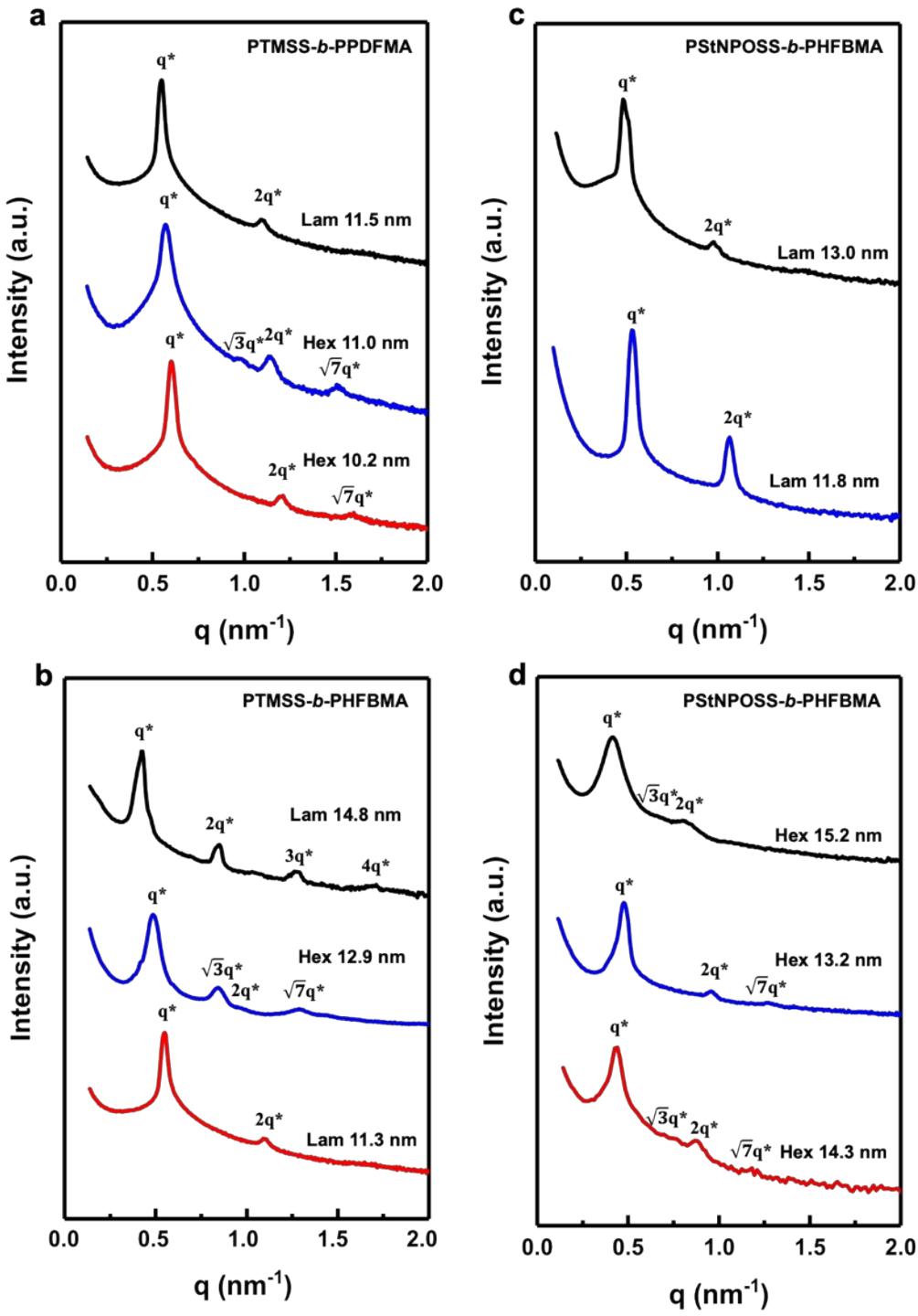

Figure S5. a) and b) were SAXS profiles of PTMSS-*b*-PPDFMA and PTMSS-*b*-PHFBMA block copolymers after annealing completion (10 h at 160 °C), respectively. c) and d) were SAXS profiles of PStNPOSS-*b*-PHFBMA block copolymers after annealing completion (1 h at 160 °C). The morphologies and *d*-spacings were presented above the end of each SAXS profile. D-spacings equaled to 2 π/q*, where q* was position of the first-order peak in SAXS.

3. Determination of χ by temperature-dependent SAXS

Equations used to fit the disordered state scattering of a block copolymer are shown below.[1, 2]

$$\mathrm{I}(q) = A/(S(q)/W(q)-2\chi)$$

$$\mathrm{S}(q) = <S_{Si,\,Si}(q)>+2<S_{Si,\,F}(q)>+<S_{F,\,F}(q)>$$

$$\mathrm{W}(q) = <S_{Si,\,Si}(q)>\cdot<S_{F,\,F}(q)>-<S_{Si,\,F}(q)>^2$$

$$<S_{X,\,X}(q)> = r_c f_X{}^2 g^{(2)}{}_X(q)$$

$$<S_{Si,F}(q)> = r_c f_{Si} f_F g^{(1)}{}_{Si}(q) g^{(1)}{}_F(q)$$

$$r_c = (v_{Si} N_{Si} + v_F N_F)/\ (v_{Si} \cdot v_F)^{1/2}$$

$$g^{(1)}{}_X(q) = \{1-[y_X(q)\cdot(Đ_X-1)+1]^{-1/(Đ_X-1)}\}/y_X(q)$$

$$g^{(2)}{}_X(q) = 2\{-1+y_X(q)+[y_X(q)\cdot(Đ_X-1)+1]^{-1/(Đ_X-1)}\}/y_X(q)^2$$

$$y_X(q) = N_X a_X{}^2/6\cdot q^2$$

$$Đ_X = M_{\mathrm{w},X}/M_{\mathrm{n},X}$$

Where *Si* = Si-containing block (PTMSS or PStNPOSS), *F* = fluorinated block (*F*, PHFBMA or PPDFMA), and *X* = Si-containing block or fluorinated block according to specific BCP system, $Đ_X$ is the dispersity index determined by GPC, a is the statistical segment length, N is volume-based degree of polymerization normalized by using 118 Å^3 as a reference volume, f is the volume fraction of two segments, and v is the molar volume calculated by bulk density of each segment.

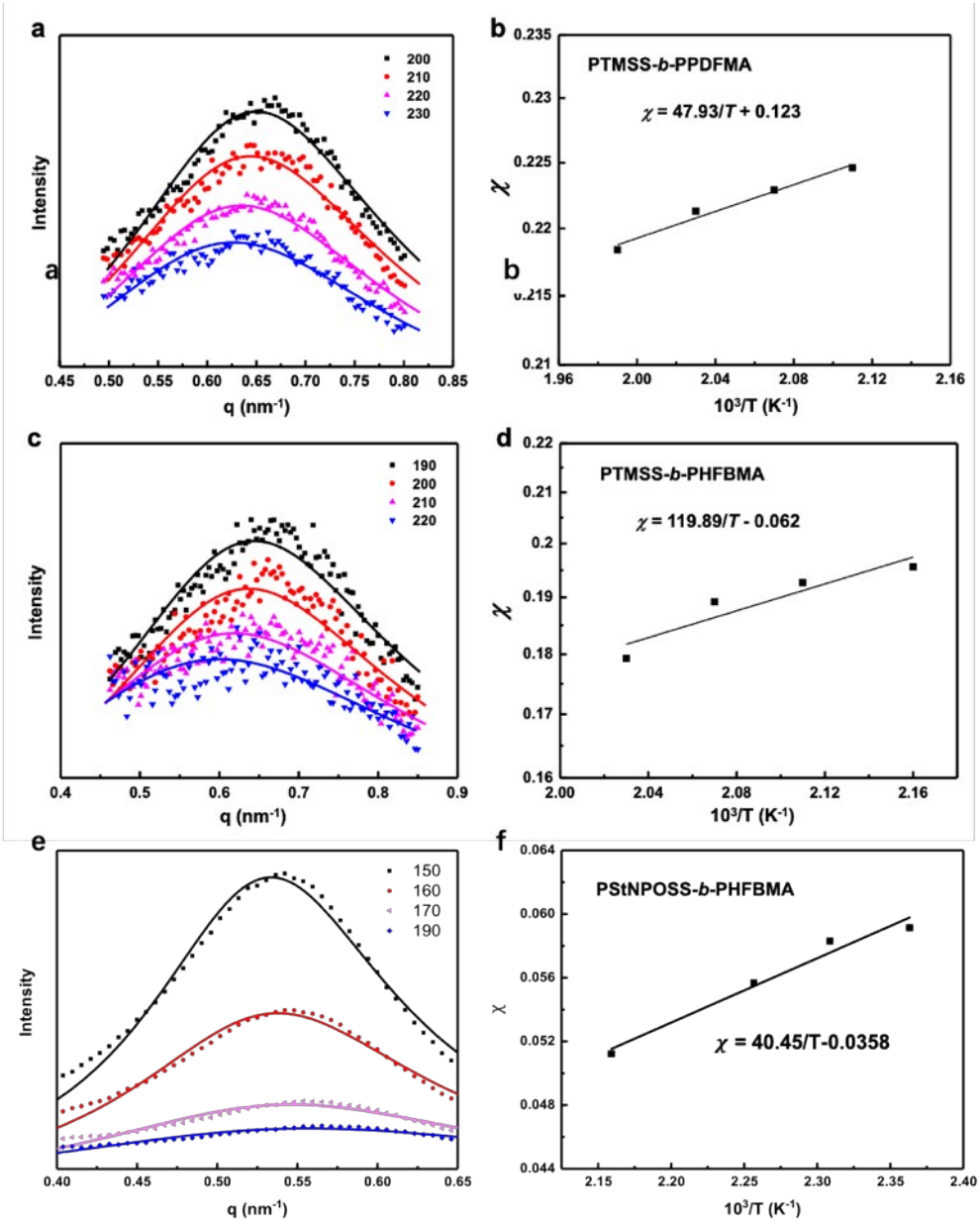

Figure S6. (a) SAXS data and fitlines for disordered PTMSS-*b*-PPDFMA at various temperatures. The best fit was obtained by changing χ as one of the adjustable parameters using Leibler's mean-field theory. (b) Temperature dependence of χ between PTMSS and PPDFMA and the corresponding best fitline. (c) to (f) are corresponding results of PTMSS-*b*-PHFBMA and PStNPOSS-*b*-PHFBMA.

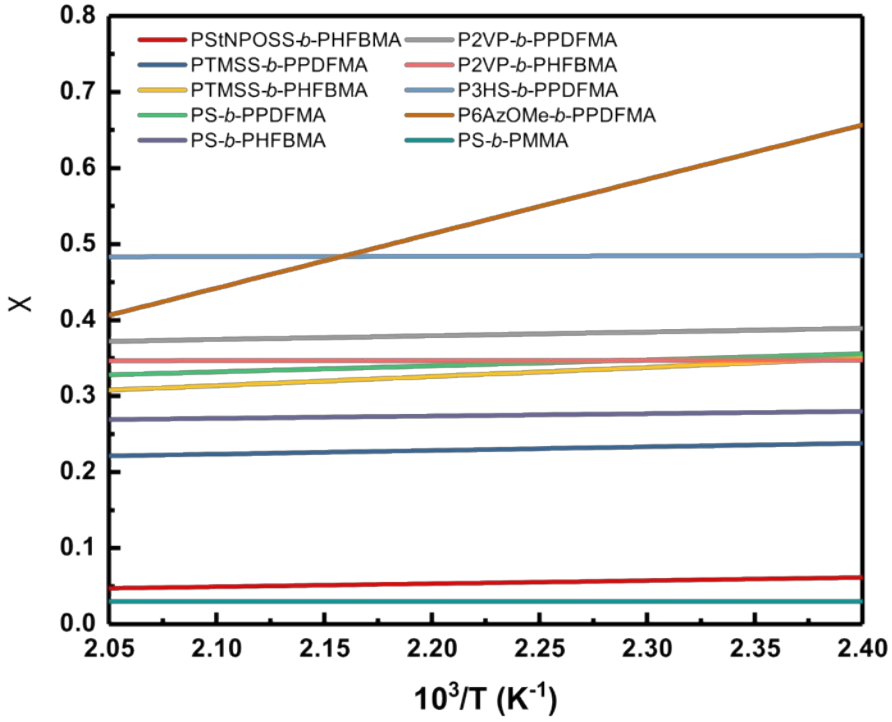

Figure S7. Temperature dependence fitline of χ value of fluorinated BCPs and conventional PS-*b*-PMMA.

Table S2. χ value of fluorinated BCPs and conventional PS-*b*-PMMA.

BCP	Relation between T and χ	χ_{eff} (@150 °C)
PStNPOSS-*b*-PHFBMA	χ = 40.45/T-0.0358	0.060
PTMSS-*b*-PPDFMA	χ = 47.93/T+0.123	0.236
PTMSS-*b*-PHFBMA	χ = 119.89/T-0.062	0.221
PS-*b*-PPDFMA[3]	χ = 78.51/T+0.167	0.353
PS-*b*-PHFBMA[3]	χ = 30.80/T+0.206	0.279
P2VP-*b*-PPDFMA[4]	χ = 48.79/T+0.272	0.387
P2VP-*b*-PHFBMA[4]	χ = 2.29/T+0.342	0.347
P3HS-*b*-PPDFMA[5]	χ = 4.4/T+0.4742	0.485
P6AzOMe-*b*-PPDFMA[6]	χ = 715.7/T-1.061	0.630
PS-*b*-PMMA	/	0.030

4. Self-assembly performance of BCPs with one POSS or TMSS block

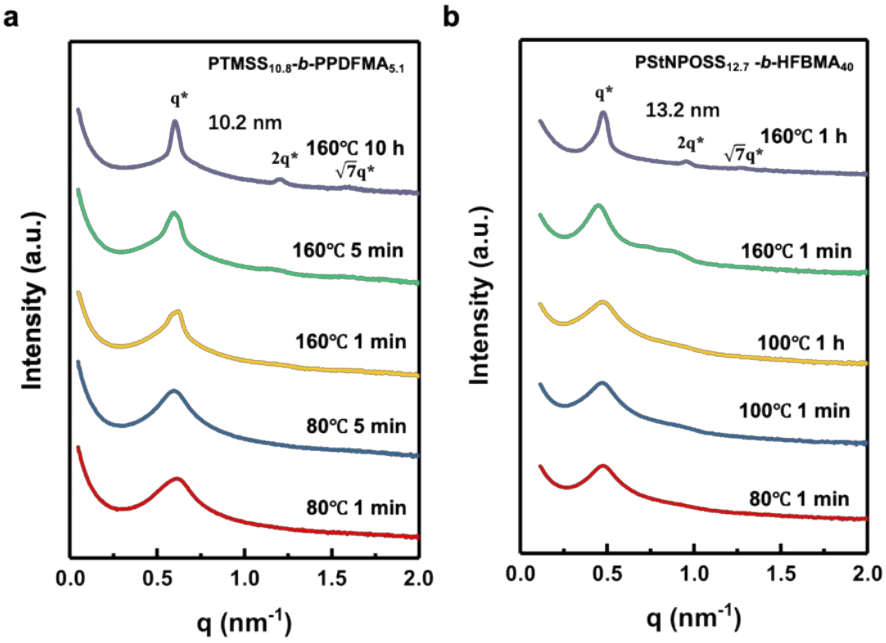

Figure S8. (a) SAXS profiles of $PTMSS_{10.8}$-b-$PPDFMA_{5.1}$ after thermal annealing at 80 °C (1 min and 5 min), 160 °C (1 min, 5 min and 10 h). (b) SAXS profiles of $PStNPOSS_{12.7}$-*b*-$PHFBMA_{40}$ after thermal annealing at 80 °C (1 min), 100 °C (1 min and 1 h) and 160 °C (1 min, 1 h).

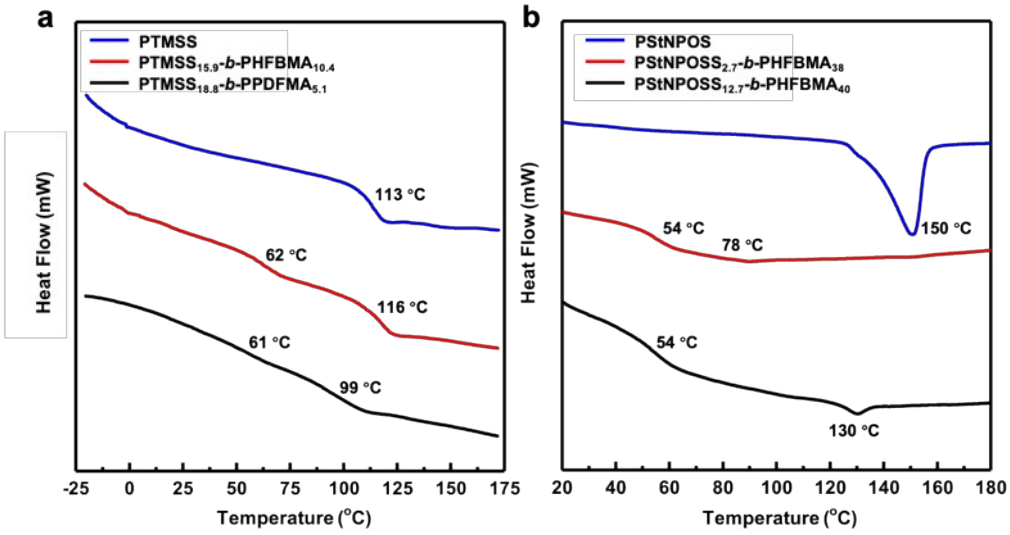

Figure S9. (a) DSC curves of $PTMSS_{18.8}$-*b*-$PPDFMA_{5.1}$ (T_g, 61 ºC and 99 ºC) and $PTMSS_{15.9}$-*b*-$PHFBMA_{10.4}$ (T_g, 62 ºC and 116 ºC) compared to PTMSS (T_g, 113 ºC) homopolymer. (b) DSC curves of $PStNPOSS_{2.7}$-*b*-$PHFBMA_{38}$ (T_g, 54 ºC and 78 ºC) and $PStNPOSS_{12.7}$-*b*-$PHFBMA_{40}$ (T_g, 54 ºC; T_m, 130 ºC) compared to PStNPOSS (T_m, 150 ºC) homopolymer.

5. Characterization of Poly(St-*co*-StNPOSS)-*b*-PHFBMA BCP

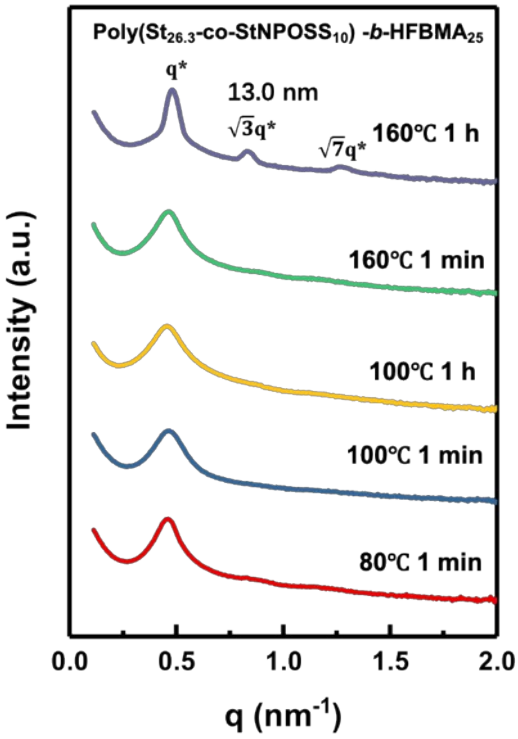

Figure S10. SAXS profiles of Poly($St_{26.3}$-*co*-$StNPOSS_{10}$)-*b*-$PHFBMA_{25}$ after thermal annealing at 80 °C (1 min), 100 °C (1 min and 1 h) and 160 °C (1 min, 1 h).

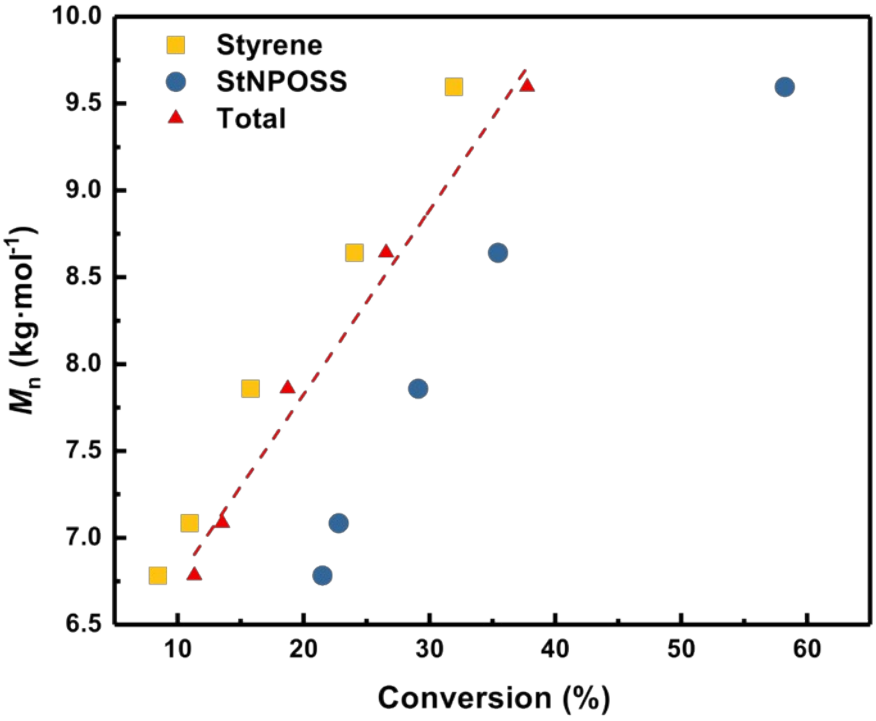

Figure S11. Styrene, StNPOSS and total monomer conversion against molecular weight in

second step RAFT polymerization of Poly(St-*co*-StNPOSS)-*b*-PHFBMA.

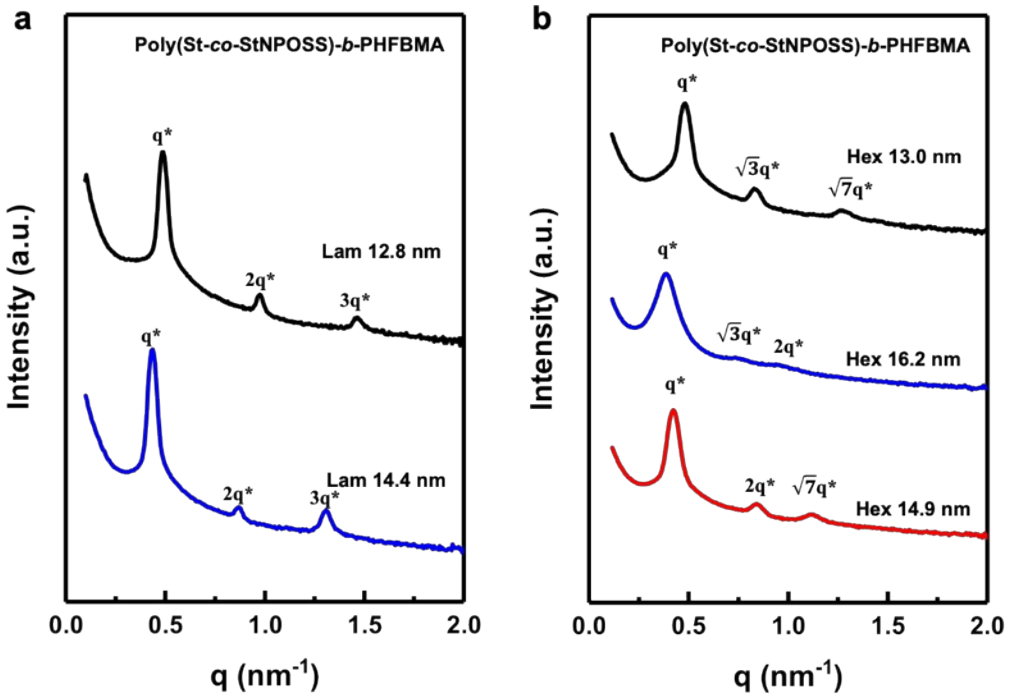

Figure S12. SAXS profiles of Poly(St-*co*-StNPOSS)-*b*-PHFBMA block copolymers after annealing completion (1 h at 160 °C). The morphologies and *d*-spacings were presented above the end of each SAXS profile. D-spacings equaled to 2 π/q*, where q* was position of the first-order peak in SAXS.

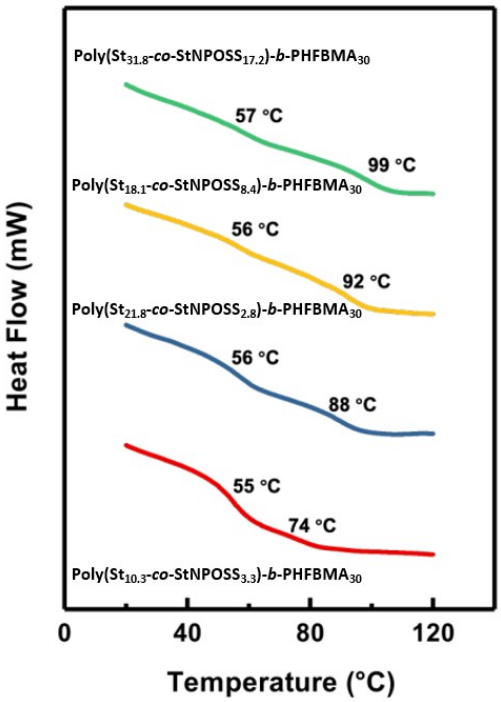

Figure S13. DSC curves of Poly (St-*co*-StNPOSS)-*b*-PHFBMA BCP samples.

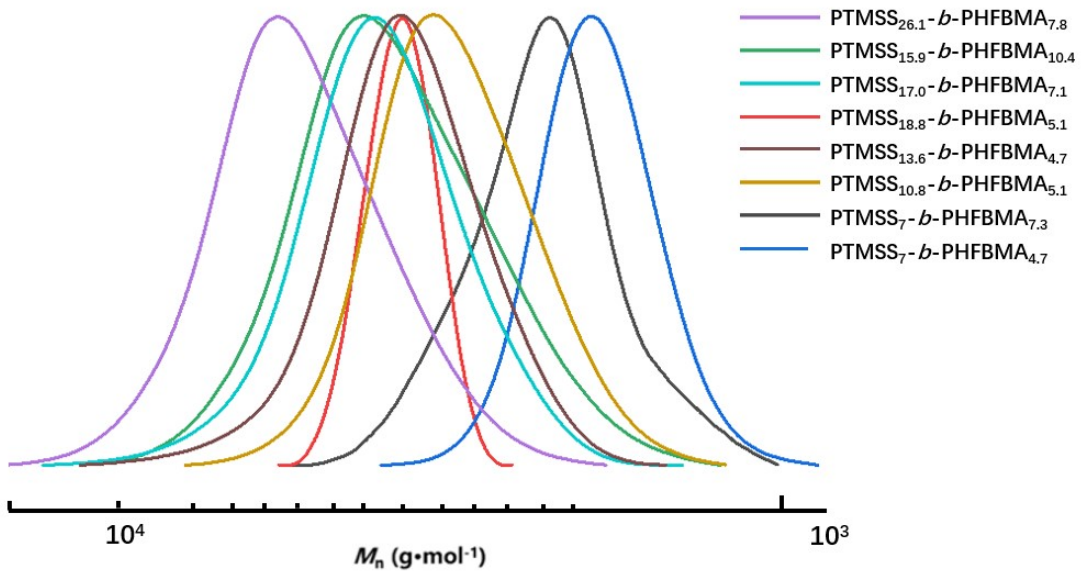

Figure S14. GPC traces of synthesized PTMSS-*b*-PHFBMA.

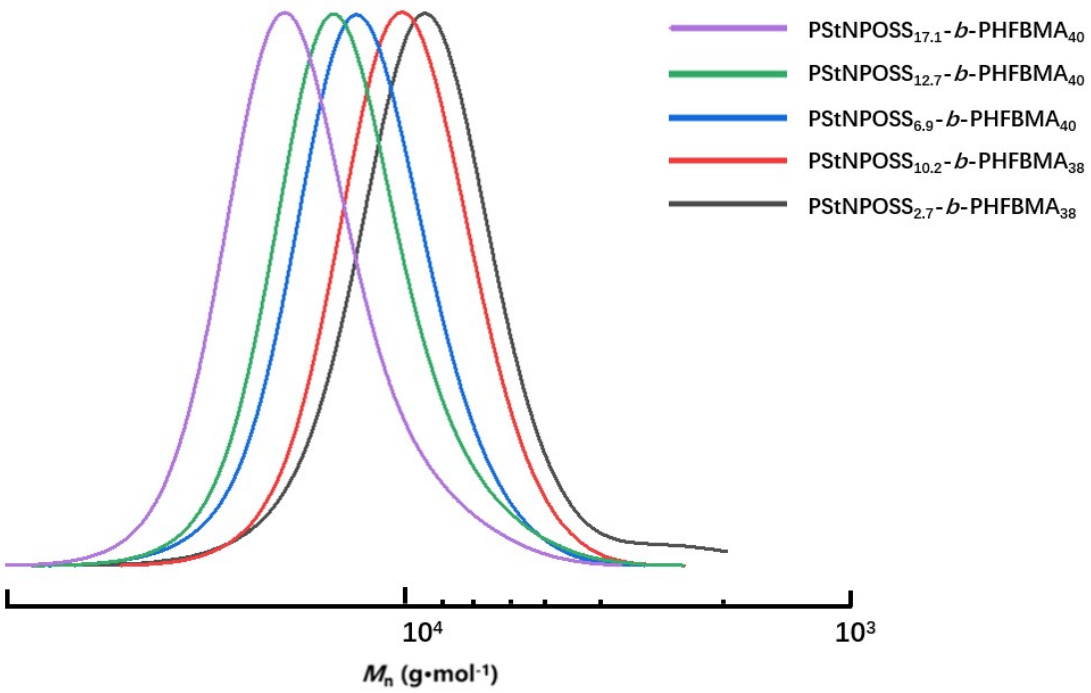

Figure S15. GPC traces of synthesized PStNPOSS-*b*-PHFBMA.

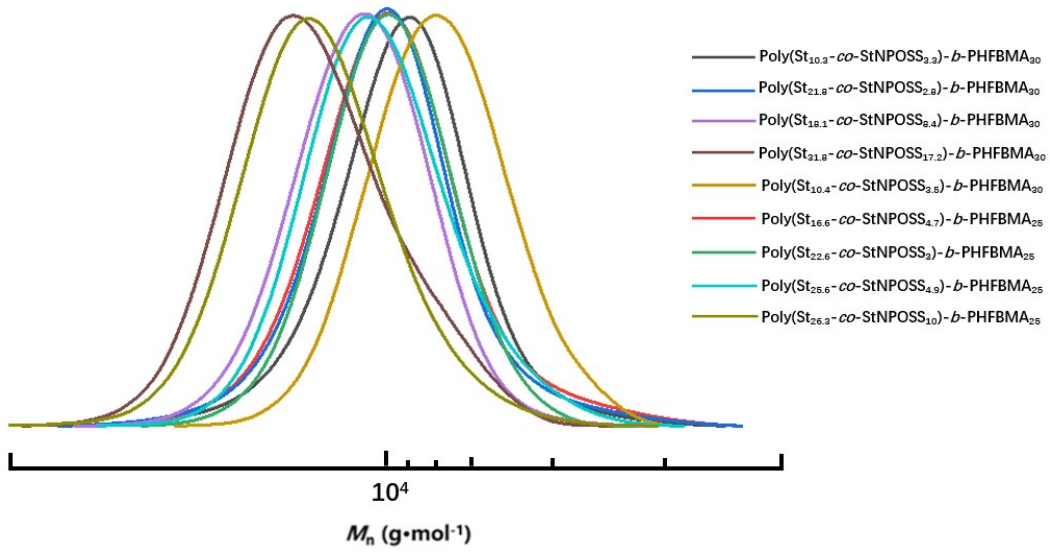

Figure S16. GPC traces of synthesized Poly (St-*co*-StNPOSS)-*b*-PHFBMA.

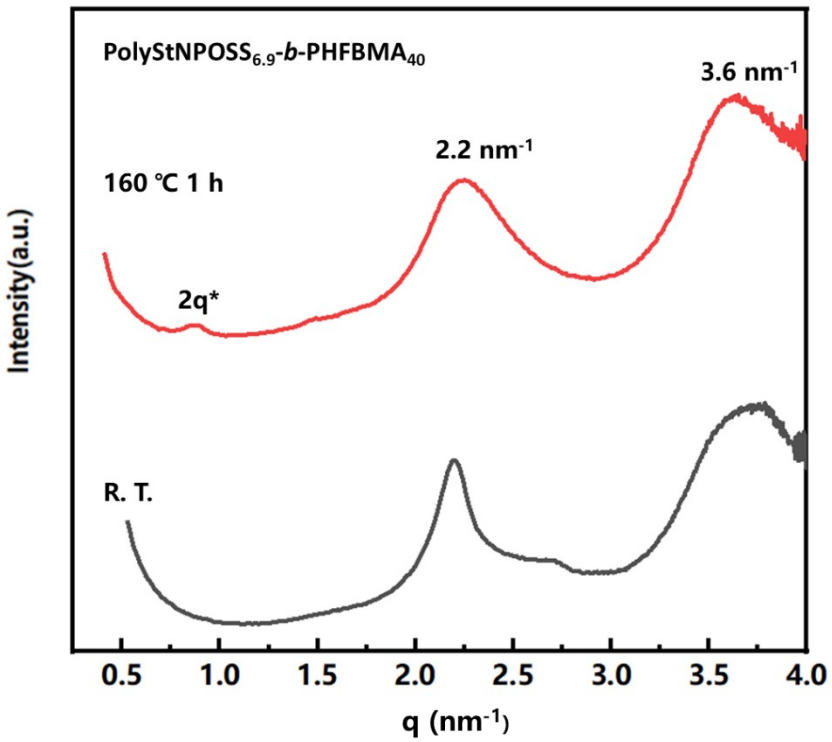

Figure S17. WAXS profiles of PolyStNPOSS$_{6.9}$-*b*-PHFBMA$_{40}$ under room temperature (black) and after 1 hour at 160 ℃, peaks positioned at 2.2 nm^{-1} and 3.6 nm^{-1} exists in both profiles.

5. Etch resistance characterization

Table S3. Polymers used for etch resistance characterization

Polymer	Si wt%	M_n[b)]	Change of Film Thickness[c)] (nm, 60 s)
PMMA	/	18.1	59.5
PS	/	3.8	34.8
PHFBMA	/	5.1	44.1
PTMSS	15.9%	3.5	18.1
Poly(St-*co*-StNPOSS)[a)]	18.5%	5.7	12.9
PStNPOSS	22.3%	9.6	6.2

a) The molar ratio between PS and PStNPOSS, calculated by ^{1}H NMR, was 2:1. b) Molecular weight was measured by GPC in THF against PS standards. c) Change of film thickness after etching for 60 s.

References

(1). Leibler, L., Theory of Microphase Separation in Block Copolymers. *Macromolecules* **1980,** 13, (6), 1602-1617.

(2). Sakamoto, N.; Hashimoto, T., Order-Disorder Transition of Low Molecular Weight Polystyrene-*block*-Polyisoprene. 1. SAXS Analysis of Two Characteristic Temperatures. *Macromolecules* **1995,** 28, (20), 6825-6834.

(3). Li, X.; Li, J.; Wang, C.; Liu, Y.; Deng, H., Fast Self-Assembly of Polystyrene-*b*-poly(fluoro methacrylate) into Sub-5 nm Microdomains for Nanopatterning Applications. *Journal of Materials Chemistry C* **2019,** 7, (9), 2535-2540.

(4). Li, X.; Deng, H., Poly(2-vinylpyridine)-*b*-poly(fluorinated methacrylate) Block Copolymers Forming 5 nm Domains Containing Metallocene. *ACS Applied Polymer Materials* **2020,** 2, (8), 3601-3611.

(5). Wang, C.; Li, X.; Deng, H., Synthesis of a Fluoromethacrylate Hydroxystyrene Block Copolymer Capable of Rapidly Forming Sub-5 nm Domains at Low Temperatures. *ACS Macro Letters* **2019,** 8, (4), 368-373.

(6). Cao, H.; Dai, L.; Liu, Y.; Li, X.; Yang, Z.; Deng, H., Methacrylic Block Copolymers Containing Liquid Crystalline and Fluorinated Side Chains Capable of Fast Formation of 4 nm Domains. *Macromolecules* **2020,** 53, (20), 8757-8764.